

# Aph-1 Associates Directly with Full-length and C-terminal Fragments of $\gamma$ -Secretase Substrates\*<sup>§</sup>

Received for publication, November 29, 2009, and in revised form, February 5, 2010. Published, JBC Papers in Press, February 9, 2010, DOI 10.1074/jbc.M109.088815

Allen C. Chen, Lucie Y. Guo, Beth L. Ostaszewski, Dennis J. Selkoe, and Matthew J. LaVoie<sup>1</sup>

From the Center for Neurologic Diseases, Brigham and Women's Hospital and Harvard Medical School, Boston, Massachusetts 02115

$\gamma$ -Secretase is a ubiquitous, multiprotein enzyme composed of presenilin, nicastrin, Aph-1, and Pen-2. It mediates the intramembrane proteolysis of many type I proteins, plays an essential role in numerous signaling pathways, and helps drive the pathogenesis of Alzheimer disease by excising the hydrophobic, aggregation-prone amyloid  $\beta$ -peptide from the  $\beta$ -amyloid precursor protein. A central unresolved question is how its many substrates bind and enter the  $\gamma$ -secretase complex. Here, we provide evidence that both the  $\beta$ -amyloid precursor protein holoprotein and its C-terminal fragments, the immediate substrates of  $\gamma$ -secretase, can associate with Aph-1 at overexpressed as well as endogenous protein levels. This association was observed using bi-directional co-immunoprecipitation in multiple systems and detergent conditions, and an  $\beta$ -amyloid precursor protein-Aph-1 complex was specifically isolated following *in situ* cross-linking in living cells. In addition, another endogenous canonical  $\gamma$ -substrate, Jagged, showed association of both its full-length and C-terminal fragment forms with Aph-1. We were also able to demonstrate that this interaction with substrates was conserved across the multiple isoforms of Aph-1 ( $\beta$ ,  $\alpha$ S, and  $\alpha$ L), as they were all able to bind  $\beta$ -amyloid precursor protein with similar affinity. Finally, two highly conserved intramembrane histidines (His-171 and His-197) within Aph-1, which were recently shown to be important for  $\gamma$ -secretase activity, are required for efficient binding of substrates. Taken together, our data suggest a dominant role for Aph-1 in interacting with  $\gamma$ -secretase substrates prior to their processing by the proteolytic complex.

$\gamma$ -Secretase is a conserved and essential intramembrane protease that processes a large and growing number of type I membrane proteins having diverse functions that include regulation of cell fate, immune recognition, cell-cell interaction, and other aspects of signal transduction (reviewed in Refs. 1, 2). Although presenilin (PS)<sup>2</sup> is thought to be the catalytic core of the prote-

ase, it does not possess autonomous proteolytic activity; several protein cofactors are required to reconstitute  $\gamma$ -secretase activity. The protease complex consists of four integral membrane proteins as follows: PS, Aph-1, nicastrin (NCT), and Pen-2, and the functional contributions of each member of the complex are still being elucidated. PS exists in the complex as a heterodimer of its N- and C-terminal fragments (NTF/CTF), each of which provides one of the two catalytic aspartates to the active site (3). NCT is the only single-transmembrane component, and its large glycosylated ectodomain, specifically residue Glu-333, has been proposed to recognize the free N termini of substrates prior to their cleavage by PS (4, 5). However, this finding is under debate, as recent work suggests that residue Glu-333 of NCT functions principally in the proper maturation of the  $\gamma$ -secretase complex (6, 7) and not in the binding of substrates *per se* (6); moreover, a recent study (8) has demonstrated that NCT is dispensable for  $\gamma$ -secretase activity in the presence of certain PS missense mutations. Pen-2 is a small two-transmembrane protein that binds to full-length PS and enables autoproteolysis of the latter into its active heterodimeric form (9–13). Aph-1 is the least well understood member of the complex. Its seven-transmembrane topology (14) and its ability to bind NCT early in  $\gamma$ -secretase assembly, as demonstrated by us and others, have suggested that it may initiate complex assembly in the endoplasmic reticulum (13, 15–19). However, whether Aph-1 performs functions in the complex beyond serving as a structural scaffold for initial component assembly, *e.g.* in the actual processing of substrates, remains unknown.

The report that NCT may bind the extreme N termini of substrate CTFs following the shedding of the ectodomains by  $\alpha$ -secretase raised the possibility that other  $\gamma$ -secretase components might serve to initially recognize the holoproteins as well as the respective CTFs. In this regard, small amounts of full-length APP and full-length Notch have been reported to be associated with  $\gamma$ -secretase (15, 20–24). Moreover, the Notch ligands, Delta and Jagged, are substrates of  $\gamma$ -secretase, and the unprocessed full-length Delta and Jagged holoproteins were also reported to interact with  $\gamma$ -secretase (25). There is biochemical evidence for the existence of at least two distinct substrate-binding sites within the  $\gamma$ -secretase complex, the catalytic site and an initial substrate-docking site (26, 27). Here, we conducted an unbiased analysis to identify which  $\gamma$ -secretase

\* This work was supported, in whole or in part, by National Institutes of Health Grants AG015379 (to D. J. S.) and AG023094 (to M. J. L.). This work was also supported by an award for Excellence in Biomedical Research from The Smith Family and Ludke Family Foundations (to M. J. L.).

§ Author's Choice—Final version full access.

§ The on-line version of this article (available at <http://www.jbc.org>) contains supplemental Figs. 1–6.

<sup>1</sup> To whom correspondence should be addressed: Center for Neurologic Diseases, Harvard Institutes of Medicine, Rm. 764, Boston, MA 02115. Tel.: 617-525-5185; Fax: 617-525-5252; E-mail: mlavoie@rics.bwh.harvard.edu.

<sup>2</sup> The abbreviations used are: PS, presenilin; A $\beta$ , amyloid  $\beta$ -peptide; APP,  $\beta$ -amyloid precursor protein; CHAPSO, 3-[(3-cholamidopropyl) dimethylammonio]-2-hydroxy-1-propanesulfonate; CHO, Chinese hamster ovary cells; DDM, dodecyl- $\beta$ -maltoside; DSP, dithiobis [succinimidylpropionate];

HEK, human embryonic kidney cells; NCT, nicastrin; NTF/CTF, N/C-terminal fragments; HA, hemagglutinin; Tricine, N-[2-hydroxy-1,1-bis(hydroxymethyl)ethyl]glycine; WT, wild type; FL, full length; TMD, transmembrane domain; DAPT, N,N-(3,5-difluorophenacetyl-L-alanyl)-S-phenylglycine t-butyl ester.

component(s) associates most clearly with substrates. We report several lines of evidence that Aph-1 can participate in the binding of full-length substrates as well as their CTFs. The interactions were observed using bi-directional co-immunoprecipitation as well as live cell cross-linking under both overexpressed and endogenous conditions. Aph-1-substrate interaction was preserved in detergents that dissociate the  $\gamma$ -secretase complex, suggesting that Aph-1 can bind to substrates directly. Importantly, similar data were obtained for the functionally unrelated  $\gamma$ -secretase substrates, Jagged and APP, suggesting that the interaction may be generalized across the many  $\gamma$ -secretase substrates. In addition, we found that the three different isoforms of Aph-1 can interact with APP in a similar manner. Finally, two conserved histidines within transmembranes 5 and 6, which were recently shown to be important for  $\gamma$ -secretase activity (28), are also involved in the interaction of Aph-1 and substrate. Our results suggest Aph-1 as a dominant factor in the initial association between substrate and protease.

## EXPERIMENTAL PROCEDURES

**Mutagenesis**—Domain-swapped and histidine mutants of *APH-1* were cloned into a pCDH Puro or pCDH Zeo vector, respectively, using a two-step PCR. A total of four primers were used per construct; N/C-terminal primers and internal primers that contained the desired mutation in-frame with the adjacent *APH-1 $\alpha$*  sequence. In the first round of PCR, two reactions would generate a 5'- and a 3'-half with a complementary 20-bp overlap containing the desired mutation. The two resulting products were added together and used as a template for the second round of PCR where extreme N/C-terminal *APH-1* primers were added. All mutants were generated in the *APH-1 $\alpha$*  isoform with a C-terminal HA tag and their sequences verified.

**Cell Culture, Transfections, and Lentiviral Transduction**—Chinese hamster ovary (CHO) cells and human embryonic kidney 293 (HEK) cells were maintained in standard medium: Dulbecco's modified Eagle's medium plus 10% fetal bovine serum, 2 mM L-glutamine, 100  $\mu$ g/ml streptomycin, and 100 units/ml penicillin. For our  $\gamma$ -30 cell line, which overexpresses human APP, PS1, Aph-1 $\alpha$ L-HA, FLAG-Pen-2, and transferrin receptor, standard medium was supplemented with G418, puromycin, Zeocin, and hygromycin, as described previously (29). Our S-1 and S-20 cell lines ( $\gamma$ -30 cells that additionally overexpress NCT-GST or NCT-V5, respectively) were propagated in  $\gamma$ -30 medium supplemented with blastocidin (30). For Jagged-1 experiments, cells were transiently transfected to express rat Jagged-1-HA (gift of G. Weinmaster), Aph-1 $\alpha$ L-GST, or both, using Lipofectamine 2000 (Invitrogen) or FuGENE 6.0 (Roche Applied Science) according to the manufacturer's protocol. Cells were harvested 36 h later in either 1% DDM for co-immunoprecipitation experiments or 1% Nonidet P-40, 0.1% SDS for cross-linking studies. All samples were protein normalized and subjected to GSH pulldowns.

For lentiviral generation of *APH-1* mutants, DNA constructs (domain-swapped in pCDH Puro Vector or histidine mutants in pCDH Zeo Vector) were co-transfected with the helper plasmid  $\Delta$ 8.9 and VSV-G. Medium containing the virus was harvested 60–72 h later and spun at 500 rpm. Virus was stored at

–80 °C. P-22 cells (29) were transduced with lentivirus containing various Aph-1 mutants following our published protocol (31). Briefly, P-22 cells were split to a confluency of 10%, and lentivirus was added to these cells supplemented with 6  $\mu$ g/ml Polybrene and extra media. Cells were infected for 60–72 h and supplemented with additional media. P-22 cells transduced with the various Aph-1 isoforms or the histidine mutants were selected with 500  $\mu$ g/ml Zeocin and propagated with standard P-22 media containing Zeocin.

**Sample Preparation**—Microsomes were generated from whole brains of wild type or APP<sup>-/-</sup> mice (32) or from E13 Sprague-Dawley rat embryos. Briefly, whole brains or embryos were extracted and Dounce-homogenized in Tris-buffered saline and then passed four times through a 27.5-gauge needle. Nuclei and cell debris were pelleted by centrifugation at 1,000  $\times$  *g* followed by a 100,000  $\times$  *g* spin to pellet microsomes. Microsomes from  $\gamma$ -30 cells, HEK cells, or mouse brains were prepared in 50 mM Hepes buffer, pH 7.0, containing either 1% CHAPSO or 1% DDM or prepared in 50 mM Tris buffer, pH 7.6, containing 150 mM NaCl, 2 mM EDTA, and 1% Nonidet P-40 or 1% Nonidet P-40 + 0.5% Triton X-100. Protease inhibitor mixture (Roche Applied Science) was added into each lysis buffer. Samples were incubated on ice for 30–60 min and centrifuged at 100,000  $\times$  *g* for 60 min to remove detergent-insoluble material. The resultant lysates were quantified using a bicinchoninic acid-based protein assay (Pierce), and all samples were normalized for protein concentration prior to immunoprecipitation, GSH pulldown, or SDS-PAGE. Typically, a protein concentration of 1.0–1.5 mg/ml was used in a volume of 800–1000  $\mu$ l per immunoprecipitation.

**Co-immunoprecipitations**—For immunoprecipitations, HA-tagged proteins were affinity-isolated with 3F10 resin (Roche Applied Science) or HA-7 resin (Sigma) and FLAG and V5-tagged proteins with M2 or V5 resins (Sigma), respectively; Jagged with a C-terminal antibody C-20 (Santa Cruz Biotechnology), and APP with 8E5 or 13G8 monoclonal antibodies (to amino acids 444–592 or 675–695 of APP695, respectively; gifts of P. Seubert, Elan PLC) or our polyclonal antibody, C9, directed against the C terminus of APP. For immunoprecipitations of endogenous APP, the antibody 13G8 was used alongside equal concentrations of a control monoclonal antibody, M2, that does not recognize endogenous proteins. Endogenous Aph-1 $\alpha$ L was immunoprecipitated with the C-terminal antibody O2C2 (Affinity Bioreagents), endogenous NCT with N1660 (Sigma), and endogenous PS1 with X81 (20) Aph-1-GST was enriched by pulldown using a commercially available GSH resin (Amersham Biosciences). Samples were normalized for protein content and precleared for 90 min, followed by incubation with the indicated antibody and protein A or protein G overnight at 4 °C. The following day, immunoprecipitations in 1% CHAPSO or 1% DDM were washed three times (15 min each) in lysis buffer. Immunoprecipitations in 1% Nonidet P-40 or 1% Nonidet P-40 + 0.5% Triton were washed more stringently, as described previously (20, 22). For Jagged antibody preabsorption experiments, 2.0  $\mu$ g/ml C-20 antibody was coupled with protein G-agarose and preabsorbed with 0 or 0.2  $\mu$ g/ml of C-20 blocking peptide at 4 °C for 4 h. Coupled complexes were then used to immunoprecipitate samples from

## Aph-1 Binds to $\gamma$ -Secretase Substrates

HEK cells transiently transfected with Jagged-1 or from endogenous E13 rat embryos.

**In Situ Live Cell Cross-linking**—Cells prepared for cross-linking experiments were washed three times in phosphate-buffered saline containing 1 mM MgCl<sub>2</sub> and 1 mM CaCl<sub>2</sub> and incubated with the indicated concentration of the thiol-cleavable cross-linker DSP (prepared from a 20 mM stock solution in DMSO; Pierce) for 30 min at room temperature, and the reaction was then quenched with 50 mM Tris buffer, pH 7.4, for 15 min. Cellular proteins were then extracted in 1% Nonidet P-40 + 0.1% SDS to completely dissociate noncross-linked protein-protein interactions. Cell lysates were then immunoprecipitated overnight with the indicated resin (3F10, HA-7, or GSH for the respective tagged proteins) or else 13G8 plus protein G-agarose (for endogenous APP) and stringently washed with three sequential 20-min washes in 0.2% Nonidet P-40 Tris-buffered saline (TBS) solution containing 500 mM NaCl, 0.2% Nonidet P-40 TBS containing 0.1% SDS or 0.2% Nonidet P-40 TBS only. Proteins were released from the resins using 2× Laemmli sample buffer without reducing agent. An aliquot was removed for probing the uncleaved protein complexes, and the remaining sample was cleaved in 50 mM dithiothreitol or 5%  $\beta$ -mercaptoethanol for 1 h at 37 °C and then analyzed by SDS-PAGE and Western blotting. For HA-7 preabsorption experiments, 100  $\mu$ g/ml HA peptide (Sigma) was preincubated with HA-7 resin prior to immunoprecipitation.

**Electrophoresis and Western Blotting**—Samples were loaded onto 4–20% Tris glycine or 10–20% Tris/Tricine gels, transferred to polyvinylidene difluoride (Millipore) or nitrocellulose membranes, and probed for various proteins according to standard Western blotting procedures. FLAG-tagged proteins were detected with monoclonal antibody, M2, or a rabbit polyclonal antibody, F7425 (both Sigma). HA-tagged proteins were detected with rat monoclonal antibody, 3F10 (Roche Applied Science). NCT was detected with either R302 (gift of D. Miller and P. Savam), mouse  $\alpha$ -NCT (BD Transduction Laboratories), or rabbit  $\alpha$ -NCT (N1660, Sigma). Holo-PS and its NTF were detected with 231f (gift of B. Yankner), Ab14 (gift of S. Gandy), anti-PS1 N-terminal (Calbiochem), or MAB1563 (Millipore). PS CTF was detected with 4627, MAB5232 (Millipore), or 13A11 (gift of P. Seubert). Aph-1 was detected with B80.3 (gift of B. De Strooper), O2C2 (Affinity Bioreagents), or  $\alpha$ -Aph-1 $\alpha$  (Zymed Laboratories Inc.), and Pen-2 was detected with anti-Pen-2 (gift of C. Haass) or UD-1 (gift of J. Nasland). Full-length APP and its CTFs were detected with CT-20 (Calbiochem), our C7, C8, or C9 antisera, or 13G8 (33). 22C11 (Millipore) was used to detect full-length APP. Jagged-1 was detected using C-terminal directed antibodies H-114 and C-20 (Santa Cruz Biotechnology). Aph-1-GST was detected using an anti-GST antibody (Amersham Biosciences). Transferrin receptor was detected with a mouse  $\alpha$ -human transferrin receptor antibody (Zymed Laboratories Inc.).

**Conditioned Media and A $\beta$  Enzyme-linked Immunosorbent Assay**—P-22 cells stably expressing various Aph-1 constructs were split into 6-well plates and grown to confluence. Cells were then conditioned with standard Dulbecco's modified Eagle's medium minus serum for 24 h. Conditioned media were isolated, spun at 1,000  $\times$  g, and stored at –80 °C. The

remaining cells were harvested in 50 mM Tris buffer, pH 7.6, containing 150 mM NaCl, 2 mM EDTA, and 1% Nonidet P-40; the protein was assayed and probed for the levels of  $\gamma$ -secretase components.

A $\beta$ -(1–40) enzyme-linked immunosorbent assays were performed using a standard A $\beta$  enzyme-linked immunosorbent assay kit from Invitrogen, following the manufacturer's protocol. Levels of A $\beta$  were normalized to protein concentration from the corresponding whole cell lysate. All data were normalized to WT Aph-1.

**Quantification**—All quantification was performed using the Odyssey infrared imaging system (LI-COR Biosciences). Only well resolved bands were included for quantitative analyses. For quantifying APP co-immunoprecipitation, levels of precipitated APP were divided by the levels of mature  $\gamma$ -secretase complex as measured by PS1 NTF. For quantifying Aph-1 co-immunoprecipitation, levels of precipitated Aph-1 were divided by their respective start levels. All data were normalized to either Aph-1 $\alpha$ L or the WT construct, which were each set to 100%. Statistical analysis was performed with PRISM version 4.03 for Windows (GraphPad Software, San Diego) using a one-way analysis of variance and Tukey's post-hoc test for pairwise comparison. All quantitative data are presented as the mean  $\pm$  S.D.

## RESULTS

**$\gamma$ -Secretase Substrate APP Co-immunoprecipitates with Aph-1 under Native and  $\gamma$ -Dissociating Conditions**—Given the multiprotein nature of  $\gamma$ -secretase, we sought to determine which  $\gamma$ -component(s) may principally participate in the key step of the association between substrate and protease. The integrity, and thus the cleavage activity, of the  $\gamma$ -secretase complex is highly sensitive to detergent conditions. Although it is stable and active in the presence of certain detergents (e.g. 1% CHAPSO or digitonin),  $\gamma$ -secretase can be completely dissociated in 1% Nonidet P-40 or be partially dissociated into two prominent and relatively stable but proteolytically inactive subcomplexes (Aph-1-NCT and PS-Pen-2) when extracted in 1% DDM (Fig. 1A) (15, 34). Importantly, the protein-protein interactions within  $\gamma$ -secretase identified using DDM for partial dissociation have been corroborated by various laboratories using other methods (11, 12, 18, 19).

We initially utilized our well characterized  $\gamma$ -30 CHO cell line (29), which stably overexpresses human PS1, Aph-1 $\alpha$ L-HA, FLAG-Pen-2, APP, and transferrin receptor. We treated these cells with the  $\gamma$ -secretase inhibitor *N*-[*N*-(3,5-difluorophenacetyl-L-alanyl)]-S-phenylglycine *t*-butyl ester) (10  $\mu$ M, 4 h; gift of M. Wolfe) to enhance detection of the C83 APP CTF;  $\gamma$ -secretase activity is augmented severalfold in  $\gamma$ -30 cells so that the levels of substrate CTFs are near the lower limits of detection in the absence of DAPT, even using sensitive antibodies. We then lysed the cells in either 1% CHAPSO (for intact  $\gamma$ -secretase) or 1% DDM (to fragment  $\gamma$ -secretase into the two subcomplexes) and immunoprecipitated the lysates for FLAG-Pen-2 or Aph-1 $\alpha$ L-HA using M2 (anti-FLAG) or 3F10 (anti-HA) affinity resins, respectively (see "Experimental Procedures"), to determine which half of the complex can bind full-length APP and/or its CTFs. Under conditions in which



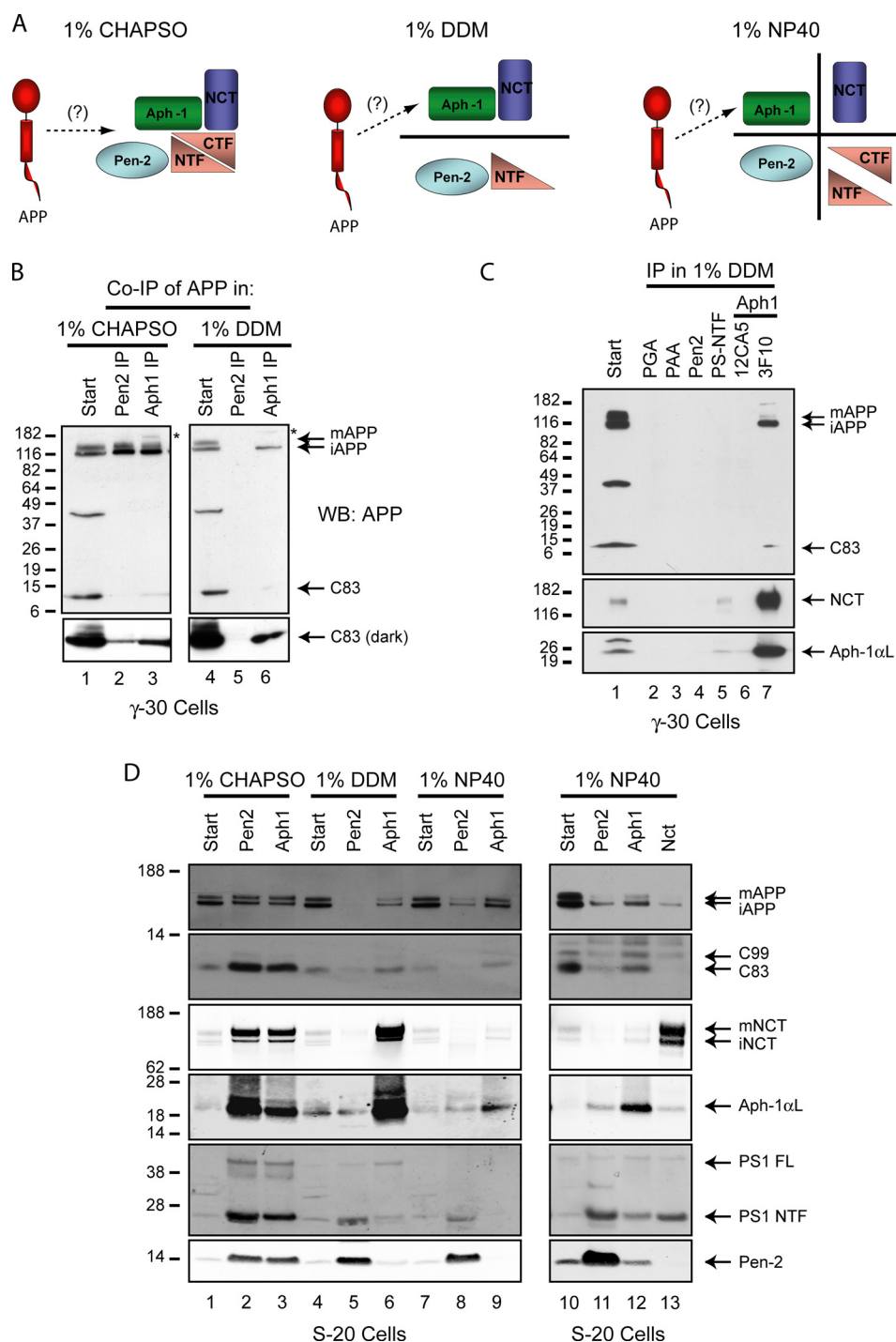


**FIGURE 1. Co-immunoprecipitation reveals an interaction between Aph-1 and the  $\gamma$ -secretase substrate APP in  $\gamma$ -30 and S-20 cells.** *A*, model depicting the integrity of the  $\gamma$ -secretase complex in 1% CHAPSO but its division into two subcomplexes in 1% DDM and into four individual components in 1% Nonidet P-40 (NP40). Dotted lines with (?) indicate the possible interactions of APP with components that we hypothesized before performing this work. *B*,  $\gamma$ -30 cells were treated with DAPT (10  $\mu$ M) for 4 h to increase C83 levels, lysed in native (1% CHAPSO) or mildly dissociating (1% DDM) detergent conditions, and immunoprecipitated for FLAG-Pen-2 or Aph-1 $\alpha$ L-HA with M2 or 3F10 affinity resins, respectively. The immunoprecipitates were probed for FL APP (*m*, mature; *i*, immature) and C83 with an affinity-purified C-terminal antibody, C9. \* denotes nonspecific band; *WB*, Western blot; *Co-IP*, co-immunoprecipitation. *C*, to test for nonspecific interactions with the resins used, DDM lysates of  $\gamma$ -30 cells were immunoprecipitated using protein G-agarose (PGA), protein A-agarose (PAA), Pen2-FLAG with M2 affinity resin, PS NTF with antibody 1563 + protein G-agarose, and Aph-1 $\alpha$ L-HA with antibody 12CA5 (anti-HA) + protein G-agarose, or 3F10 resin (anti-HA). Immunoprecipitates (IP) were blotted for APP (C9), NCT (N1660), and Aph-1 (O2C2). *D*, to determine whether the Aph-1 interaction with APP is dependent on NCT and to determine the relative contributions of Pen-2, Aph-1 (*D*, left panel), and NCT (*D*, right panel) to substrate binding, S-20 cells were lysed in native (CHAPSO), partially dissociating (DDM), or completely dissociating (Nonidet P-40 (NP40)) conditions and immunoprecipitated for FLAG-Pen-2, Aph-1 $\alpha$ L-HA, or NCT-V5 with M2, HA-7, or V5 resin, respectively. Immunoprecipitates were probed for the presence of FL APP (22C11) and CTFs (C7) and the components of  $\gamma$ -secretase: NCT (N1660), PS1 (MAB1563), Aph-1 $\alpha$ L-HA (3F10), and FLAG-Pen-2 (F7425, Sigma).

## Aph-1 Binds to $\gamma$ -Secretase Substrates

$\gamma$ -secretase is intact and active (1% CHAPSO), both full-length (FL) APP and its ectodomain-shed CTF (C83) co-immunoprecipitated with FLAG-Pen-2 and with Aph-1 $\alpha$ L-HA (Fig. 1B, lanes 2 and 3, respectively). However, when the complex was partially dissociated by 1% DDM, no APP came down with the Pen-2-PS subcomplex (*i.e.* by M2 immunoprecipitation), whereas both FL-APP and C83 still co-immunoprecipitated with the Aph-1-NCT subcomplex (*i.e.* by 3F10 immunoprecipitation) (Fig. 1B, lanes 5 and 6). To exclude that this result was due to significant differences in the binding capacities of our anti-FLAG (M2) and anti-HA (3F10) resins, we stripped and reprobed the blots to determine whether the degree of co-immunoprecipitation was comparable with these two resins. In native conditions (1% CHAPSO), the M2 and 3F10 resins brought down similar amounts of complex-associated NCT, holo-PS, and PS NTF (data not shown).

To address the specificity of the APP-Aph-1 co-immunoprecipitation, we examined the ability of several resin and antibody combinations to immunoprecipitate APP in the 1% DDM lysates of the  $\gamma$ -30 cells. Protein A-agarose alone, protein G-agarose alone, M2-FLAG resin, 1563 (anti-PS1 NTF), 12CA5 (anti-HA), and 3F10 (anti-HA) were each tested for their ability to co-immunoprecipitate APP from the 1% DDM lysates of  $\gamma$ -30 cells (Fig. 1C). Only in the case of 3F10 (directed against the HA tag on Aph-1) did we detect an interaction with APP and its CTF (Fig. 1C, lane 7). Surprisingly, 12CA5, a monoclonal antibody targeted against HA, did not detectably co-immunoprecipitate APP as 3F10 did. However, upon stripping and reprobing the membrane for Aph-1, we found that only 3F10, not 12CA5, had significantly enriched for Aph-1 (Fig. 1C, bottom panel, compare lanes 6 and 7), explaining the lack of APP co-immunoprecipitation using 12CA5.

Previous studies had reported an interaction between PS and various  $\gamma$ -secretase substrates in cells (20, 22, 23); therefore, we decided to further examine whether PS alone might participate in an association with APP.  $\gamma$ -30 lysates were immunoprecipitated for PS1 with an N-terminally directed antibody (X81) in either 1% CHAPSO or 1% DDM and probed for the presence of APP. Under non-denaturing conditions (1% CHAPSO), X81 strongly immunoprecipitated both holo-PS and PS NTF, and also the other components of  $\gamma$ -secretase, as expected. X81 also brought down both holo-APP and C83 (supplemental Fig. 1, lane 2). In the DDM lysates, immunoprecipitation with X81 brought down even more holo-PS and PS NTF, and low levels of NCT but no Aph-1. Here, there was no co-immunoprecipitation of FL APP or C83 with PS (supplemental Fig. 1, lane 4). The latter result suggests that although PS can associate with both Aph-1 and APP when the  $\gamma$ -complex is intact (*i.e.* under native conditions), Aph-1 plays the principal role in the interaction with APP.

The NCT ectodomain has been reported to bind the extreme N terminus of recently shed substrates (4), suggesting that it is also involved in substrate binding. Although our  $\gamma$ -30 cells have a relatively high level of endogenous NCT, we wanted to provide equal opportunity for NCT and Aph-1 to interact with substrates. Therefore, we turned to our S-20 cell line, which are  $\gamma$ -30-based cells that also stably overexpress NCT-V5 and have a 5-fold increase in  $\gamma$ -secretase activity over  $\gamma$ -30 cells (35). S-20

cells were lysed under native (CHAPSO), partially dissociating (DDM), or fully dissociating (Nonidet P-40) conditions (as illustrated in Fig. 1A), and then immunoprecipitated for FLAG-Pen-2 (M2 immunoprecipitation) or Aph-1 $\alpha$ L-HA (HA-7). Consistent with what we observed in our  $\gamma$ -30 cells (Fig. 1, B and C), APP in the S-20 cells associated with both the Pen-2 and Aph-1 resins under native conditions (Fig. 1D, lanes 2 and 3) but only with the Aph-1 resin in 1% DDM (Fig. 1D, lanes 5 and 6). In 1% DDM, we were able to see the Pen-2-PS NTF subcomplex (Fig. 1D, lane 5) and the Aph-1-NCT subcomplex (Fig. 1D, lane 6), as reported previously (15, 34). Under completely dissociating conditions of 1% Nonidet P-40, the M2 and HA-7 resins predominantly enriched for only FLAG-Pen-2 or Aph-1-HA, respectively; however, the HA-7 resin co-immunoprecipitated full-length APP and its CTFs (Fig. 1D, lanes 8 and 9) even though it failed (as expected) to co-immunoprecipitate NCT. These data suggest that Aph-1, under  $\gamma$ -secretase denaturing conditions and in the absence of NCT, can maintain its interaction with the substrate APP.

To make a direct comparison between Aph-1 and NCT as regards their affinities for APP, S-20 cells were lysed in 1% Nonidet P-40 and immunoprecipitated for FLAG-Pen-2 (M2), Aph-1-HA (HA-7), and NCT-V5 (V5). Only Aph-1 resin was able to robustly pull down APP (Fig. 1D, lanes 11–13). There were low amounts of binding of APP to both the Pen-2 and NCT resins, which may be due to the low levels of Aph-1 that were still associated with these two resins in 1% Nonidet P-40 (Fig. 1D, lanes 11–13). Even in these  $\gamma$ -secretase denaturing conditions, we detected some of the overexpressed PS NTF being co-immunoprecipitated with all three resins; however, the levels of APP enrichment mirrored the levels of Aph-1 immunoprecipitation and not that of PS NTF, suggesting that Aph-1 is the primary component responsible for binding APP. This low level of association between PS and Aph-1 in Nonidet P-40 may explain the previous observation of an interaction between APP with PS (20).

The results so far demonstrate that in all conditions tested, native, partially dissociating, and fully dissociating, APP associates most robustly with the  $\gamma$ -secretase component, Aph-1 (results diagrammed in Fig. 1A). The association of Aph-1 with APP is not due to the indirect pull down of  $\gamma$ -secretase complexes, because under denaturing conditions (1% Nonidet P-40), where  $\gamma$ -secretase is dissociated into its individual components, we still observe this interaction, supporting the notion that Aph-1 may associate directly to APP and is the principal  $\gamma$ -component in substrate binding.

*Aph-1 Can Be Cross-linked to the Substrate APP in Living Cells*—As an independent confirmation of the above co-immunoprecipitation data supporting an interaction between Aph-1 and APP, we examined this apparent association using the thiol-cleavable, membrane-permeant cross-linker, DSP, providing a detergent-independent approach to validation. Cultured  $\gamma$ -30 cells were cross-linked *in situ* with increasing concentrations of DSP. The cells were then lysed in a 1% Nonidet P-40, 0.1% SDS buffer to denature  $\gamma$ -secretase and dissociate any noncross-linked protein interactions. The lysates were subjected to HA immunoprecipitation to pull down Aph-1-bound proteins, and the cross-linked immunoprecipitated material

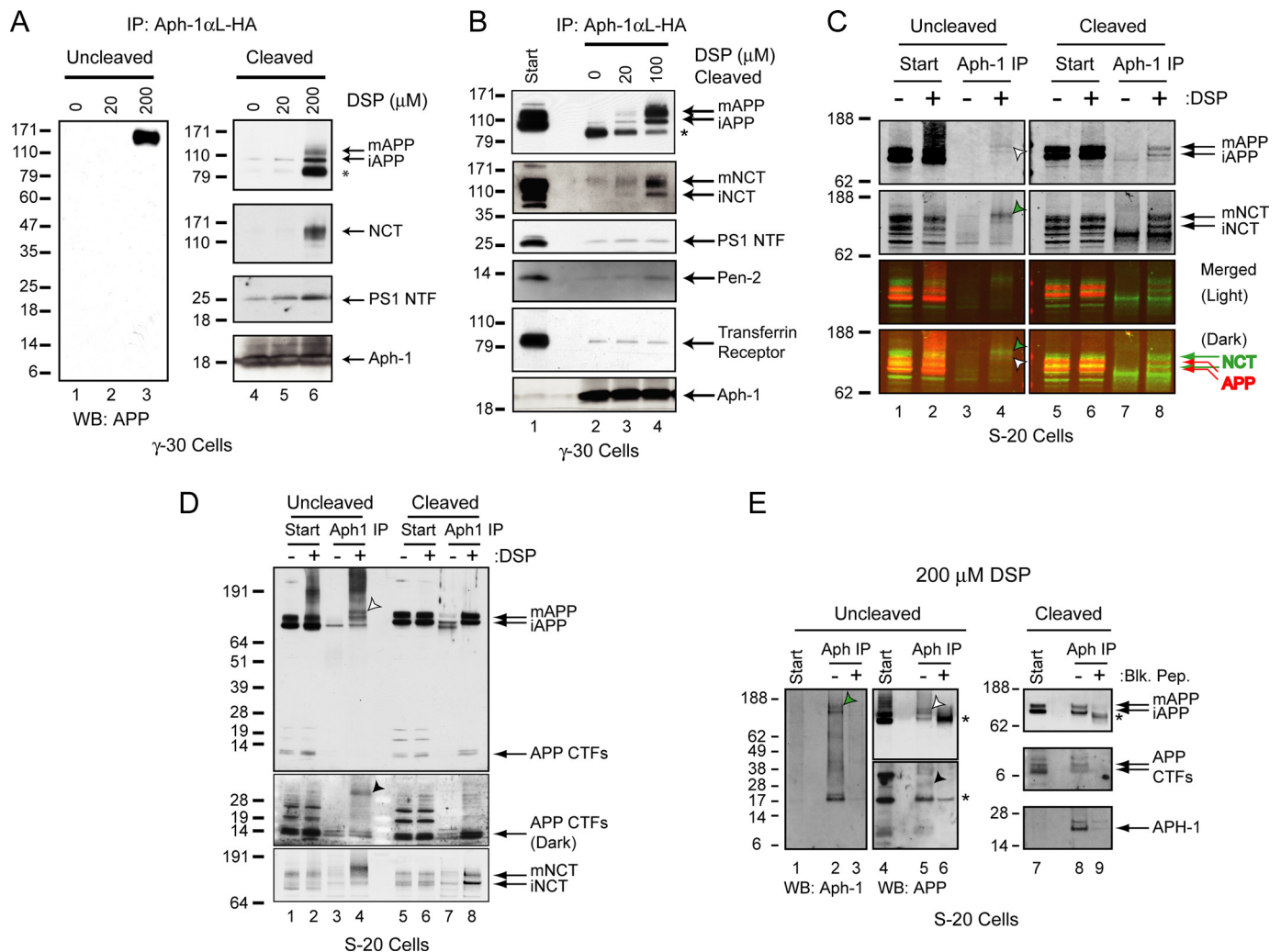


**FIGURE 2.  $\gamma$ -Secretase substrate APP can be specifically cross-linked to Aph-1 in living  $\gamma$ -30 and S-20 cells.** Live cultures of  $\gamma$ -30 cells (A and B) or S-20 cells (C–E) were treated with the thiol-cleavable cross-linker DSP at increasing concentrations and lysates (1% Nonidet P-40 + 0.1% SDS) immunoprecipitated (IP) for Aph-1 $\alpha$ L-HA (with 3F10 or HA-7). **A**, precipitates were probed prior to cleavage (left panel) for APP (affinity purified C9) or else following cleavage of the cross-linker by dithiothreitol (right panel) for APP, NCT (N1660), PS NTF (Ab14), and Aph-1 $\alpha$ L-HA (3F10). WB, Western blot. **B**, as a control for specificity, transferrin receptor (Zymed Laboratories Inc.), a type II membrane protein stably overexpressed in the  $\gamma$ -30 cells, was also probed in an independent experiment for its ability to associate with Aph-1 $\alpha$ L-HA. **C**, S-20 cells were treated with 200  $\mu$ M DSP, immunoprecipitated for Aph-1 with HA-7 resin, and probed for FL APP (22C11; red channel) and NCT (N1660; green channel) before (left panel) and after (right panel) cleavage of the DSP cross-linker. White triangle identifies an uncleaved complex immunoreactive for FL APP at  $\sim$ 150 kDa. Green triangle identifies an uncleaved complex immunoreactive for NCT. Superimposing the two images (bottom two panels: light exposure on top and stronger exposure on bottom) reveals that the NCT and FL APP immunoreactive bands migrate as two distinct complexes. **D**, same as in C but cells were probed with a C-terminal directed APP antibody (CT-20). White triangle identifies an uncleaved APP-Aph-1 complex at  $\sim$ 150 kDa. Black triangle identifies an uncleaved APP CTF-Aph-1 complex at  $\sim$ 35 kDa. **E**, S-20 cells were treated with DSP and immunoprecipitated for Aph-1 with HA resin (–) or HA resin that was preabsorbed with HA peptide (+). Cross-linked complexes were analyzed uncleaved (left panels) or cleaved (right panels) for association with Aph-1 or APP. White triangle identifies an uncleaved APP-Aph-1 complex at  $\sim$ 150 kDa. Black triangle identifies an uncleaved APP CTF-Aph-1 complex at  $\sim$ 35 kDa. Green triangle identifies a band believed to be a NCT-Aph-1 heterodimeric complex. \*, nonspecific band.

was probed by Western blotting. At a concentration of 200  $\mu$ M DSP, we found a single, discrete band immunoreactive for APP in the Aph-1 precipitates (Fig. 2A, left panel). The molecular mass of this band ( $\sim$ 150 kDa) was consistent with the molecular mass of FL APP ( $\sim$ 120 kDa) + Aph-1 ( $\sim$ 25 kDa) and was not compatible with the predicted molecular mass of a NCT-Aph-1-APP tripartite complex ( $>$ 270 kDa).

When the immunoprecipitated material was cleaved by reduction with dithiothreitol, we observed a DSP dose-dependent increase in the amount of FL APP that had been cross-linked *in situ* to Aph-1 in the intact cells (Fig. 2A, right panel). In the vehicle control (Fig. 2A, right panel, 0), we found no evidence of APP interacting with Aph-1 under the stringent wash-

ing conditions used (Nonidet P-40/SDS buffer) (Fig. 2A, lane 4). Consistent with previous data from several laboratories supporting a direct interaction between Aph-1 and NCT, NCT was cross-linked to Aph-1 in a dose-dependent manner (Fig. 2A, right panel). We were able to reproduce these data at lower concentrations of DSP (100  $\mu$ M) (Fig. 2B), and we observed little or no dose-dependent enrichment of PS NTF or Pen-2, suggesting that these proteins are apparently not in close proximity to the Aph-1-APP complex or cannot be cross-linked with this particular cross-linker under the low concentrations used. These data are consistent with a recent publication that studied the interactome within  $\gamma$ -secretase using the same exact cross-linker, DSP (36). In that study, the authors were able to identify



## Aph-1 Binds to $\gamma$ -Secretase Substrates

an interaction of Aph-1 with NCT and also with PS CTF; they did not identify an interaction with Pen-2 or PS NTF. These data support the notion that Aph-1 is in particularly close proximity to the substrate APP, because PS NTF and Pen-2, which are known components of the  $\gamma$ -secretase complex, were not cross-linked to Aph-1.

All of the components thus far examined (with the exception of NCT) are stably overexpressed in the  $\gamma$ -30 cells. Therefore, it was important to confirm that the ability to cross-link Aph-1 with APP was specific and not an artifact of overexpressing several hydrophobic integral membrane proteins in the same cell. Although PS NTF and Pen-2, which are members of the intact  $\gamma$ -secretase complex, served as important negative controls above (Fig. 2, A and B), we proceeded to examine the transferrin receptor, which is also overexpressed in the  $\gamma$ -30 cell line but is a type II protein and therefore not a substrate of  $\gamma$ -secretase (37). We found no evidence of specific transferrin receptor binding to Aph-1 on the same blot (Fig. 2B). A dark exposure is intentionally provided to illustrate the minimal background binding of transferrin receptor to the resin, with no change in the presence of DSP. Importantly, we were able to demonstrate the cross-linking between Aph-1 and APP when the APP immunoprecipitation was performed with antibodies targeting either its ectodomain or its cytoplasmic domain (supplemental Fig. 2A).

Next, we sought to compare the binding of substrates to Aph-1 versus NCT via *in situ* cross-linking in live S-1 cells (*i.e.*  $\gamma$ -30-based cells that also stably co-express NCT-GST (30)) (supplemental Fig. 2B). In the presence of DSP, NCT associated with a very small amount of FL-APP but not its CTF (supplemental Fig. 2B, lanes 2 and 3). Aph-1, however, clearly associated with both APP FL and CTFs in a DSP-dependent manner (supplemental Fig. 2B, lanes 4 and 5), again suggesting that Aph-1 is the principal  $\gamma$ -component participating in substrate binding. The very small amount of full-length APP that came down with NCT is likely due to the low levels of Aph-1 associated with NCT (supplemental Fig. 2B, lane 3).

To determine whether the cross-linked Aph-1-APP complexes we identified in Fig. 2, A and B, also contained NCT, we utilized our S-20 cells that overexpress NCT. Using 200  $\mu$ M DSP to cross-link live S-20 cells and then immunoprecipitate for Aph-1 $\alpha$ L-HA with the HA-7 resin, we were able to reproduce our findings from the  $\gamma$ -30 cells (Fig. 2, A and B) and detect a similar band at  $\sim$ 150 kDa with an ectodomain directed antibody, 22c11, suggesting that this uncleaved complex consists of Aph-1 and FL APP (Fig. 2C, lane 4, marked with *white triangle*). We were also able to detect a complex of Aph-1 and nicastrin at about that same region (marked with *green triangle*). Superimposing images of these two bands demonstrated that they are two distinct complexes as follows: an Aph-1-APP and an Aph-1-NCT complex (Fig. 2C, lane 4, bottom two panels), and not a trimeric complex of APP CTF-Aph-1-NCT (because the 22c11 APP ectodomain antibody would not detect the APP CTF). Upon reduction and cleavage of the cross-linker, we observed the appearance of FL APP and NCT that had been cross-linked to Aph-1 (Fig. 2C, lane 8). Repeating the same experiment but instead using a C-terminal directed APP antibody, CT-20, for detection, we were able to identify the same 150-kDa band (Fig.

2D, lane 4, marked with a *white triangle*); in addition, upon a darker exposure, we were able to now detect a band at  $\sim$ 35 kDa, which we believe to be a complex of Aph-1 and APP CTFs (marked with a *black triangle*). After reduction by  $\beta$ -mercaptoethanol, we saw the disappearance of the 150-kDa band and the appearance of FL APP (Fig. 2D, compare lanes 4 and 8). The same was observed for the 35-kDa band, where cleavage of the cross-linker resulted in the appearance of APP CTFs at the expense of the 35-kDa band (Fig. 2D, compare lanes 4 and 8). We were able to detect both the holo-APP/Aph-1 and the APP-CTF/Aph-1 cross-linked products at DSP concentrations as low as 25  $\mu$ M (data not shown).

As a control for immunoprecipitation specificity, we performed similar experiments as in Fig. 2, C and D, but the cross-linked samples were immunoprecipitated for Aph-1 with an HA resin versus an HA resin that was preabsorbed with HA peptide. When immunoprecipitated samples were analyzed for APP with the cross-linker intact (uncleaved), we observed the same  $\sim$ 150 kDa (marked with a *white triangle*) and  $\sim$ 35 kDa (marked with a *black triangle*) APP immunoreactive bands that we saw previously (Fig. 2E, lane 5, compare with Fig. 2, C and D, lanes 4), which we believe to be a holo-APP-Aph-1 and an APP-CTF-Aph-1 complex, respectively. We were also able to detect a NCT-Aph-1 complex (data not shown). When we blotted for Aph-1, we detected the monomeric Aph-1 protein at  $\sim$ 20 kDa and a smear above it, the latter representing all proteins cross-linked to Aph-1 (Fig. 2E, lane 2). At  $\sim$ 150 kDa, c-Aph-1 complex (marked with a *green triangle*); the APP-Aph-1 complex is likely masked beneath these bands. Preincubation with the HA-blocking peptide prevented the immunoprecipitation of Aph-1 with the HA resin (Fig. 2E, compare lanes 2 and 3) and also caused the disappearance of the APP (compare lanes 5 and 6) and NCT (data not shown) immunoreactive complexes, indicating that these cross-linked bands contain Aph-1 and are dependent on its immunoprecipitation. When the cross-linker was cleaved, we detected the co-immunoprecipitation of full-length APP as well as its CTFs, which all disappeared in the presence of blocking peptide (Fig. 2E, lanes 8 and 9).

*Interaction between Aph-1 and APP and Its CTF Occurs at Endogenous Expression Levels*—In view of the above results in transfected cells, we sought to validate the interaction between Aph-1 and APP under endogenous conditions. Untransfected HEK cells were lysed in various detergents (1% CHAPSO, 1% DDM, 1% Nonidet P-40 or 1% Nonidet P-40 + 0.5% Triton X-100), and endogenous APP was immunoprecipitated with a monoclonal antibody directed against its C terminus (13G8) and blotted for endogenous Aph-1 (Fig. 3A). In all detergents tested, 13G8 consistently co-precipitated a small amount of endogenous Aph-1, whereas equal concentrations of a control monoclonal antibody (M2) did not. No NCT was detected in the immunoprecipitates of endogenous APP in the HEK cells, consistent with the data obtained in  $\gamma$ -30 cells (data not shown), further suggesting a principal role for Aph-1 in substrate binding. These results suggest that Aph-1 and APP can associate under endogenous expression levels in HEK cells. We were also able to validate this interaction using *in situ* live cell cross-linking under endogenous levels in both HEK (Fig. 3B) and HeLa cells (data not shown), where we detected the co-immu-

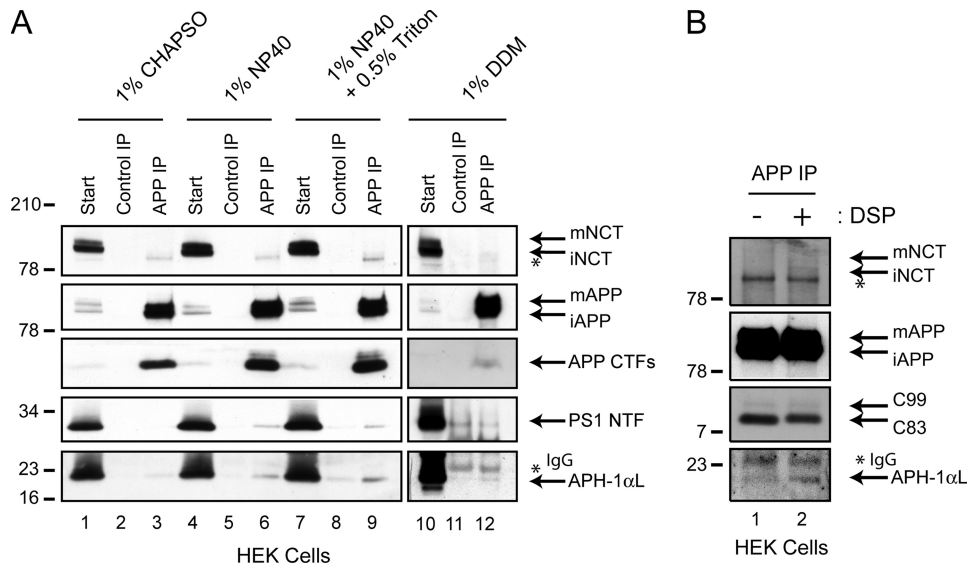


**FIGURE 3. Interaction between Aph-1 and APP is conserved under endogenous expression levels in HEK cells.** *A*, untransfected HEK293 cells were lysed in the indicated buffers, precleared, and immunoprecipitated (IP) for APP with a C-terminal directed antibody, 13G8, or a control antibody, M2. Immunoprecipitates were blotted for the indicated proteins; NCT (N1660, Sigma), APP FL and CTF (C9), PS1 NTF (231f), and Aph-1 (B80.3, lanes 1–9 or O2C2, lanes 10–12). NP40, Nonidet P-40. *B*, untransfected HEK cells were cross-linked with DSP (or DMSO as a control), lysed in a 1% Nonidet P-40/SDS buffer, and immunoprecipitated for APP with 13G8. Immunoprecipitated complexes were blotted for Aph-1 (B80.3), NCT (N1660), and APP (C9).

noprecipitation of Aph-1 (but not NCT) with APP only in the presence of the cross-linker DSP. These data demonstrate that the APP-Aph-1 interaction occurs under endogenous expression levels in HEK cells.

**Interaction between Endogenous Aph-1 and  $\gamma$ -Secretase Substrates Occurs *In Vivo***—Next, we asked whether the interaction between endogenous Aph-1 and APP was detectable *in vivo* in wild type mouse brains. Microsomal fractions from whole mouse brains were isolated and solubilized in 1% CHAPSO and immunoprecipitated for Aph-1. We were able to detect co-immunoprecipitation of APP (and other  $\gamma$ -secretase components) at endogenous levels (Fig. 4A). To determine which component within  $\gamma$ -secretase associated most readily with APP *in vivo*, we solubilized mouse brain microsomes in 1% Nonidet P-40 to dissociate the complex. Samples were immunoprecipitated for either Aph-1 $\alpha$ L (O2C2), NCT (N1660), PS1 NTF (X81), or protein A-agarose as a control (Fig. 4B). Immunoprecipitation with antibody O2C2 enriched for Aph-1 $\alpha$ L but no NCT in the Nonidet P-40 detergent; however, it was able to co-immunoprecipitate APP (Fig. 4B, lane 3). Robust immunoprecipitations of endogenous NCT or endogenous PS1 NTF did not co-immunoprecipitate APP, further supporting all of our earlier evidence that Aph-1 plays the major role in binding substrate. Next, we solubilized brain microsomes in various detergents (1% CHAPSO, 1% DDM, or 1% Nonidet P-40) and examined the interaction by performing the reverse immunoprecipitation. The solubilized membranes were immunoprecipitated for APP with monoclonal antibody 13G8 and blotted for co-immunoprecipitation of Aph-1. Similar to what we observed in untransfected HEK cells (Fig. 3A), endogenous Aph-1 was co-immunoprecipitated with endogenous APP, whereas a control antibody (M2) did not bring down detectable levels of Aph-1 (Fig. 4C). As an important control for immunoprecipitation specificity, the same experiments were repeated in APP WT

versus APP knock-out ( $-/-$ ) mouse brains (Fig. 4D). The immunoprecipitation for APP (13G8) co-precipitated Aph-1 in WT but, as expected, not in APP $^{-/-}$  mouse brains in both CHAPSO and Nonidet P-40 detergents (Fig. 4D). Interestingly, no PS or NCT was detected via co-immunoprecipitation with APP, further suggesting a dominant role of Aph-1 in substrate interaction. Taken together, our data indicate that a specific interaction between Aph-1 and APP can be observed at endogenous protein levels in brain tissue.

**Jagged-1, Another  $\gamma$ -Secretase Substrate, Associates with Aph-1 in a Manner Similar to APP**—We next sought to determine whether the role of Aph-1 in APP substrate binding may generalize to other substrates of  $\gamma$ -secretase. Jagged is a ligand of the Notch receptor that

was previously shown by us and others to be cleaved in an  $\alpha$ -secretase-like fashion to generate a C-terminal, membrane-anchored fragment that is then processed by  $\gamma$ -secretase (25, 38). We transiently transfected CHO cells to express either Jagged-1-HA, Aph-1 $\alpha$ L-GST, or both and then harvested the cells in 1% DDM and subjected the lysates (Fig. 5A, lanes 1–3) to GSH pulldowns to enrich for Aph-1. Only when both Jagged and Aph-1-GST were co-expressed did we detect FL Jagged and Jagged CTF (the immediate  $\gamma$ -secretase substrate) in the GSH pulldowns (Fig. 5A, lanes 4–6), demonstrating a specific interaction between Jagged and Aph-1, consistent with the APP data.

We then performed *in situ* cross-linking of live cells using 100  $\mu$ M DSP, a low concentration that was sufficient for cross-linking APP and Aph-1 in our previous experiments (Fig. 2). CHO cells were transiently transfected to express either Jagged or Aph-1 or both (Fig. 5B, lanes 1–3). Only when Jagged was co-expressed with Aph-1-GST and cross-linker had been applied did we observe the presence of the Jagged species in the GSH pulldowns (Fig. 5B, lanes 4–6), consistent with a specific association of FL Jagged and its CTF with Aph-1.

Because of the hydrophobicity of Aph-1 and its tendency to aggregate, we sought to confirm this interaction with endogenous Aph-1. Wild type HEK cells were transiently transfected with Jagged-1-HA and immunoprecipitated for Jagged-1 with an HA-7 resin or a C-terminal directed antibody, C20 (Fig. 5C). Both the HA-7 and C20 immunoprecipitates enriched for Jagged-1 and also co-immunoprecipitated endogenous Aph-1, whereas a control immunoprecipitation (protein A/G) did not bring down detectable levels of Aph-1. No detectable NCT was found to co-immunoprecipitate with Jagged-1.

To demonstrate the specificity of our immunoprecipitations, HEK cells were transfected with Jagged-1-HA and immunoprecipitated with 2.0  $\mu$ g/ml of the C-20 Jagged antibody that was



## Aph-1 Binds to $\gamma$ -Secretase Substrates

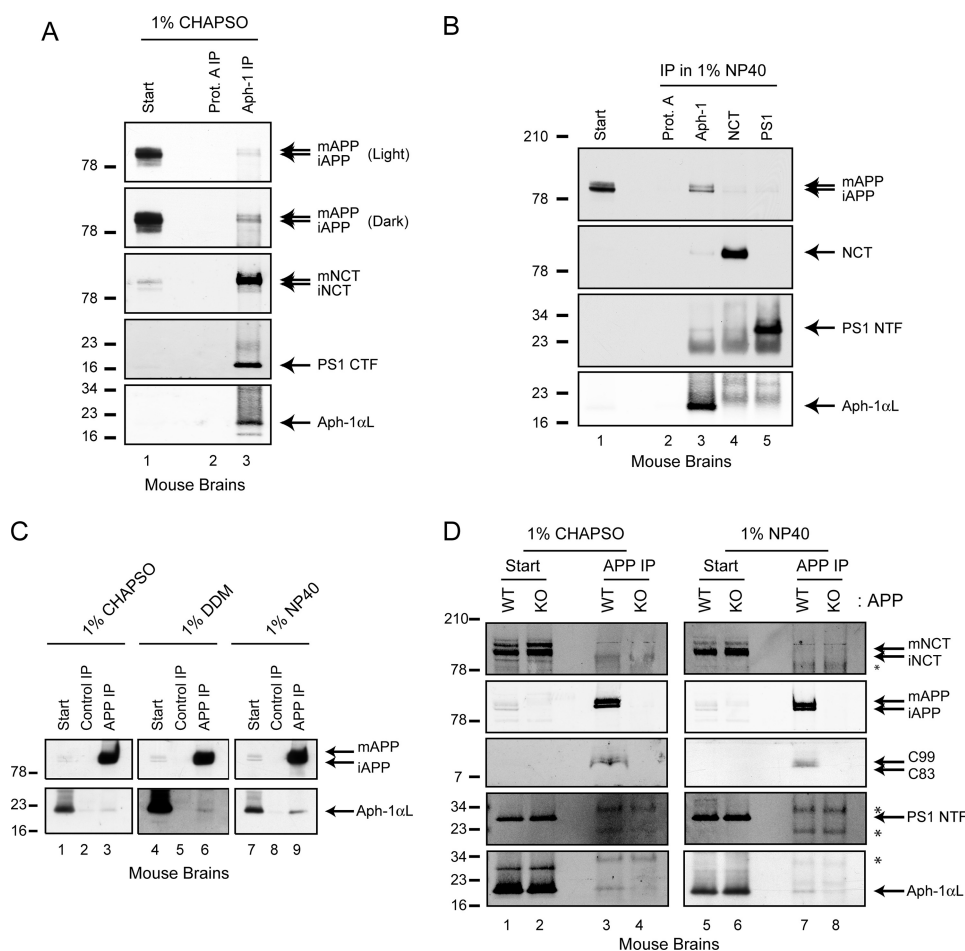


**FIGURE 4. Interaction between Aph-1 and  $\gamma$ -secretase substrates occurs *in vivo* in mouse brains.** *A*, microsomes were isolated from wild type mouse brains, solubilized in CHAPSO, and immunoprecipitated (IP) for Aph-1 $\alpha$ L with O2C2 or as a control protein A only. Immunoprecipitated samples were probed for APP (22C11), NCT (BD Transduction Laboratories), PS1-CTF (13A11), and Aph-1 $\alpha$ L (O2C2). *B*, same as in *A*, however, microsomes were solubilized in 1% Nonidet P-40 and immunoprecipitated for Aph-1 (O2C2), NCT (N1660), or PS1 (X81). The precipitates were blotted for APP (22C11), NCT (BD Transduction Laboratories), PS1 NTF (Ab14), and Aph-1 (O2C2). *C*, microsomes were isolated from wild type mouse brains, solubilized in the indicated detergents, immunoprecipitated for APP with 13G8 or equal concentrations of a control antibody (M2), and blotted for Aph-1 (O2C2) and APP (C9). *D*, microsomes from APP<sup>+/+</sup> (WT) or APP<sup>-/-</sup> (KO) mouse brains were solubilized in 1% CHAPSO (*left panel*) or 1% Nonidet P-40 (*right panel*) and immunoprecipitated with the APP antibody 13G8. Resulting precipitates were probed for APP (C9), NCT (N1660), PS1 (231f), and Aph-1 (O2C2).

preabsorbed with 0.2  $\mu$ g/ml blocking peptide. When Jagged-1 was immunoprecipitated with C-20, it brought down Aph-1 as seen previously (Fig. 5D, lane 6); however, when preabsorbed with a blocking peptide, Jagged was not immunoprecipitated, and no Aph-1 was co-immunoprecipitated (Fig. 5D, lane 7). In addition, Aph-1 was not brought down from the lysates of HEK cells that were not transfected with Jagged-1 (Fig. 5D, lane 5).

Next, we wanted to validate whether the interaction between Aph-1 and Jagged also occurred under completely endogenous expression levels *in vivo*, as we had shown for APP (Fig. 4). Microsomes were prepared from E13 rat embryos, which were previously shown by us and others to have robust expression of Jagged-1 (25, 39). Isolated microsomes were solubilized in 1% CHAPSO, immunoprecipitated for Jagged-1, and blotted for Aph-1. Consistent with the overexpression data, we were able to observe an interaction between endogenous Jagged-1 and endogenous Aph-1, whereas protein A/G-agarose alone did not enrich for Aph-1 (Fig. 5E). In addition, NCT was not co-immu-

noprecipitated with Jagged-1 (Fig. 5E, bottom panel). This interaction was specific to Jagged immunoprecipitation as no Aph-1 was co-immunoprecipitated when the immunoprecipitating antibody was preabsorbed with a blocking peptide (Fig. 5F, compare lanes 2 and 3). These experiments demonstrate that the endogenous Aph-1-Jagged interaction is not a result of nonspecific binding.

**Various Aph-1 Isoforms Interact with APP in a Similar Manner—**There exist two Aph-1 homologues in humans (Aph-1 $\alpha$  and Aph-1 $\beta$ ) and multiple splice variants for Aph-1 $\alpha$  (Aph-1 $\alpha$ S, Aph-1 $\alpha$ M, and Aph-1 $\alpha$ L). With two homologues of PS (PS1 and PS2), there are multiple distinct  $\gamma$ -secretase complexes that can be assembled (40). All our data to this point have examined the Aph-1 $\alpha$ L isoform. A recent study (41) reported that the various isoforms of Aph-1, specifically the  $\alpha$  and  $\beta$ , have different biochemical and physiological properties. We sought to determine whether the other isoforms of Aph-1 could also associate with substrate and whether they have different affinities for the  $\gamma$ -substrate APP.

We generated stable lines that express Aph-1 $\beta$ , Aph-1 $\alpha$ S, or Aph-1 $\alpha$ L in our P-22 cells, which overexpress APP, PS1, and Pen-2; with a high basal level of NCT, Aph-1 is the limiting cofactor for complex assembly in P-22 cells (29). To determine

whether the various Aph-1 isoforms can incorporate into  $\gamma$ -secretase and thus increase complex assembly and activity, we analyzed these stable cell lysates (CHAPSO) for markers of mature complex and levels of APP CTFs. All Aph-1 isoforms tested were able to increase the levels of mature NCT and PS1 NTF (markers of mature complex) while decreasing the levels of APP CTF (Fig. 6A) suggesting that they can all increase both assembly and activity of the complex. Interestingly, Aph-1 $\beta$  did not lead to as dramatic an increase in mature NCT or PS NTF levels as Aph-1 $\alpha$ ; instead it was associated with immature NCT and holo-PS. However, we were able to demonstrate that all the isoforms of Aph-1 associated with other members of  $\gamma$ -secretase by co-immunoprecipitation (supplemental Fig. 3).

Next, to determine whether the various isoforms of Aph-1 can interact with APP and its CTFs, we performed co-immunoprecipitation experiments. P-22/Aph-1 isoform-specific stable transfectants were treated with the  $\gamma$ -inhibitor, DAPT

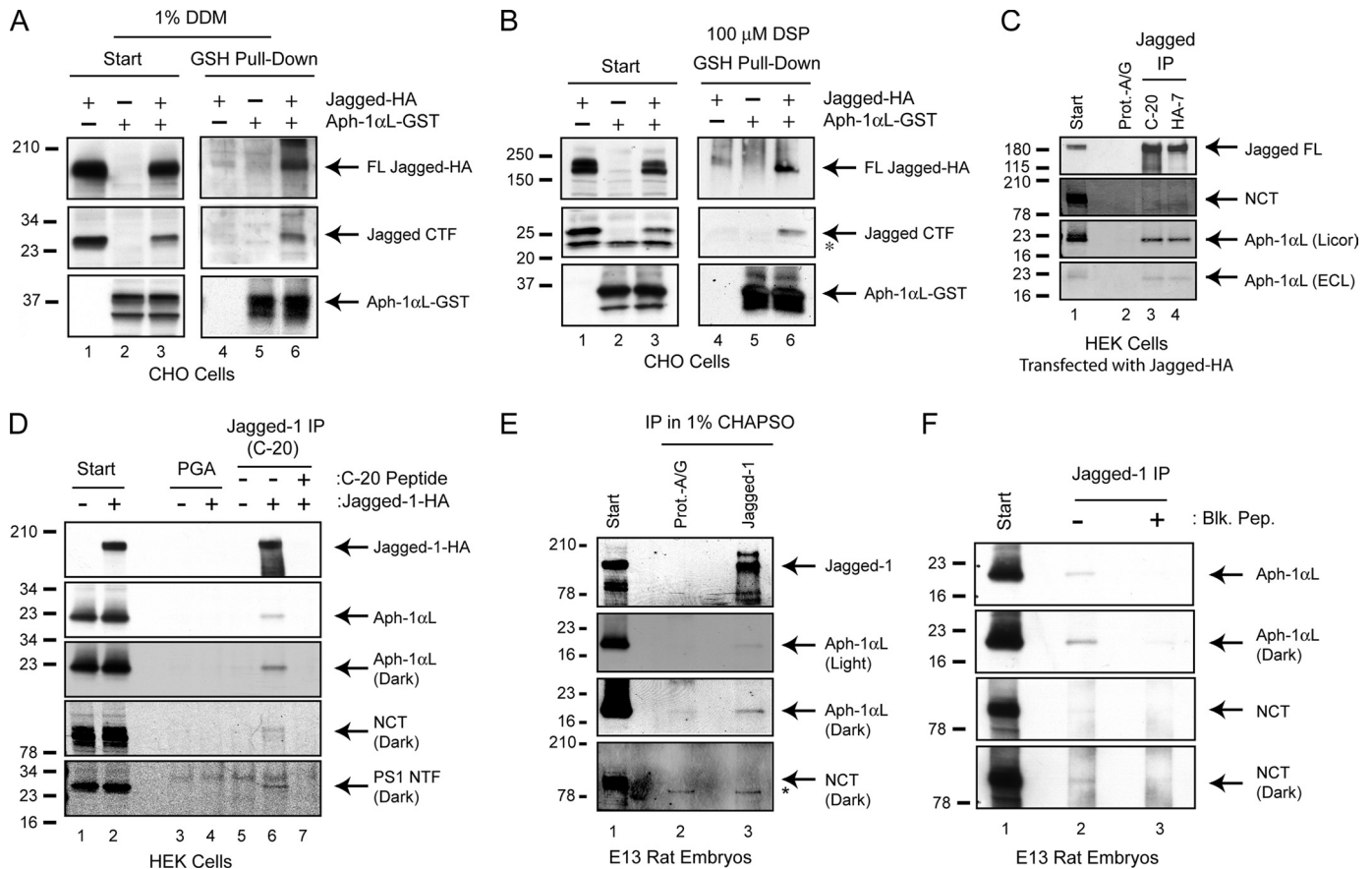


**FIGURE 5. Jagged-1, another  $\gamma$ -secretase substrate, interacts with Aph-1 in both overexpressed and endogenous systems.** *A*, CHO cells were transiently transfected with Jagged-1 HA, Aph-1-GST, or both. Cells were lysed directly in 1% DDM (*left panel*), subjected to GSH-resin pull-downs, and probed for co-pull-down (*right panel*). *B*, similarly transfected CHO cells were either directly lysed (*left panel*) or subjected to *in situ* cross-linking with DSP (100  $\mu$ M) as in Fig. 2 and probed by Western blot (*right panel*). *C*, HEK cells were transiently transfected with Jagged-1-HA, lysed in CHAPSO, and immunoprecipitated for Jagged-1 with a C-terminal directed antibody, C-20 (Santa Cruz Biotechnology), or HA-7 resin. Resulting immunoprecipitates were probed for Jagged-1-HA (3F10), Aph-1 $\alpha$ L (O2C2), and NCT (BD Transduction Laboratories). *D*, HEK cells transiently transfected with Jagged-1-HA were immunoprecipitated with C-20 antibody that was preabsorbed (or not) with a blocking peptide. *E*, microsomes isolated from E13 rat embryos were harvested in 1% CHAPSO and immunoprecipitated for Jagged-1 (C-20, Santa Cruz Biotechnology). The precipitates were blotted for Aph-1 (O2C2), Jagged-1 (H-114, Santa Cruz Biotechnology), and nicastrin (N1660, Sigma). *F*, microsomes from E13 rat embryos in 1% CHAPSO were immunoprecipitated with 2.0  $\mu$ g/ml of a Jagged antibody (C-20) preabsorbed with 0.0 or 0.2  $\mu$ g/ml of a blocking peptide, then blotting for Aph-1 (O2C2) and NCT (BD Transduction Laboratories).

(2  $\mu$ M), to increase the levels of APP CTFs, followed by lysis in CHAPSO and immunoprecipitation for Aph-1. We were able to detect the association of APP with each isoform of Aph-1, and this varied as a function of Aph-1 expression level, *e.g.* Aph-1 $\alpha$ S bound the least APP, as it was the poorest expressed (Fig. 6B). Quantifying the levels of holo-APP that co-immunoprecipitated with Aph-1 revealed that there was no significant difference between the various isoforms of Aph-1 (Fig. 6C); the levels of co-immunoprecipitated APP were corrected for the levels of Aph-1 incorporated into  $\gamma$ -secretase by normalizing to PS NTF levels. A similar lack of difference among the three Aph-1 isoforms was obtained when we normalized the APP co-immunoprecipitation levels to the Aph-1 expression level itself (data not shown).

Next, we performed the reverse co-precipitation; we immunoprecipitated APP with a C-terminal directed antibody (C9) and blotted for the co-immunoprecipitation of Aph-1. Consistent with the above data, the association with APP correlated with the relative expression of each Aph-1 isoform (Fig. 6D).

*Conserved Histidine Residues within TM5 and TM6 Are Involved in Substrate Binding*—We next sought to identify the region within Aph-1 responsible for the interaction with substrates. Because of the multiple hydrophobic domains of Aph-1, we hypothesized that the Aph-1-substrate interaction occurred within the transmembrane domains (TMDs) of Aph-1. We performed domain-swapping mutagenesis following a previously published protocol (11) in which the TMDs of Aph-1 were replaced with those of an unrelated protein. Unfortunately, all of our transmembrane domain-swapped mutants failed to incorporate stably into  $\gamma$ -secretase complexes, preventing a sound analysis of the association with substrate ([supplemental Fig. 4](#)).

Recently, two histidine residues within TMD5 or -6 of Aph-1 were shown to be important for  $\gamma$ -secretase catalytic activity (28). In that work, when histidine residues 171 and 197 were exchanged for lysine, these mutants were able to incorporate into  $\gamma$ -secretase, but the complexes formed were inactive. We hypothesized that these residues might be involved in the substrate binding we had observed. Aph-1 $\alpha$ L-HA constructs were

## Aph-1 Binds to $\gamma$ -Secretase Substrates

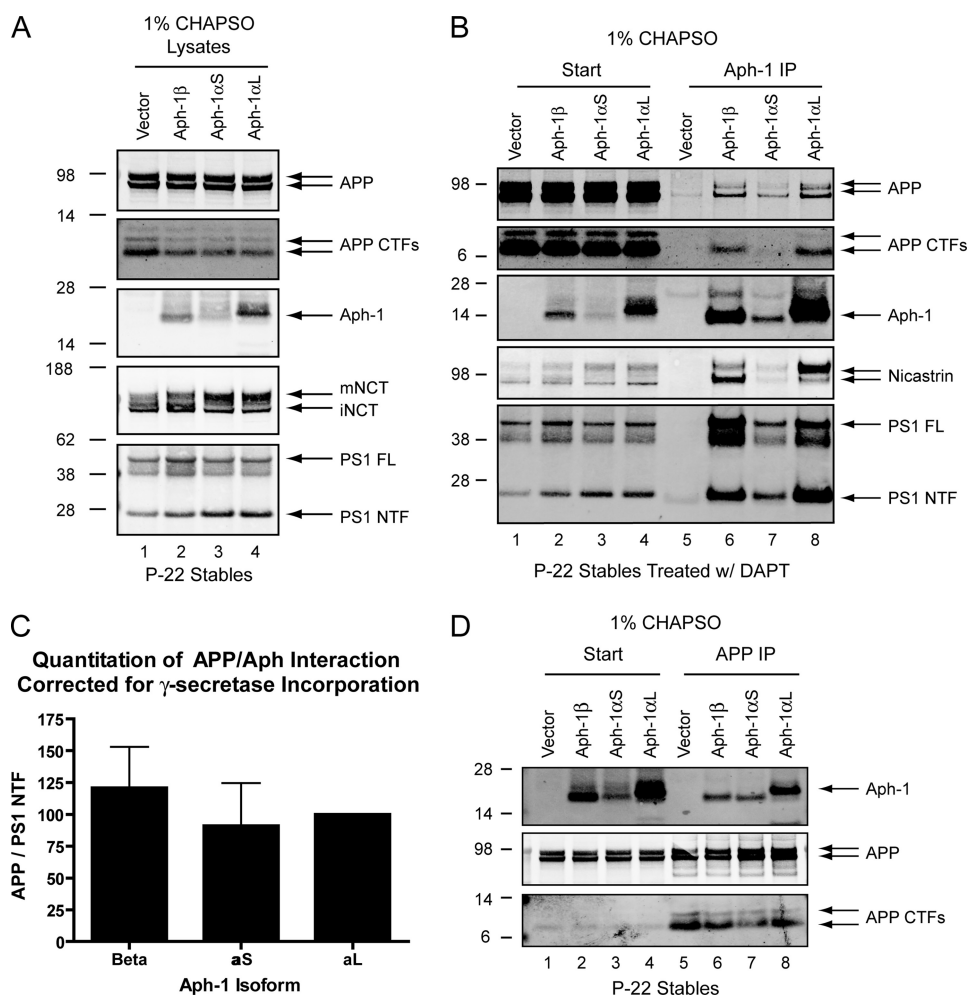


**FIGURE 6. Multiple isoforms of Aph-1 ( $\beta$ ,  $\alpha$ S, and  $\alpha$ L) interact with the substrate, APP, in a similar manner.** *A*, stable cell lines expressing the various Aph-1 isoforms containing a C-terminal HA tag were generated in P-22 cells (CHO cells that stably overexpress APP, PS1, and FLAG-Pen-2). Stable cells were lysed in 1% CHAPSO and analyzed for expression of Aph-1 (3F10); entry into the  $\gamma$ -complex was via maturation of NCT (N1660) and PS1 NTF ( $\alpha$ -PS1 NT, Calbiochem) levels; and an increase in  $\gamma$ -secretase activity was via a decrease in APP CTF (C7) levels. *B*, to determine whether the various Aph-1 isoforms can interact with APP and its CTFs, cells were treated with the potent  $\gamma$ -secretase inhibitor, DAPT (2  $\mu$ M), lysed in CHAPSO, and immunoprecipitated (IP) for Aph-1 (HA-7 resin, Sigma) and analyzed for Aph-1 (3F10) and co-immunoprecipitation of APP (C7), NCT (N1660), and PS1 NTF ( $\alpha$ -PS1 NT, Calbiochem). *C*, samples from *B* along with numerous replicates ( $n = 6$ ) were quantitated for the levels of APP co-immunoprecipitation. Aph-1 $\beta$  and Aph-1 $\alpha$ S bound APP  $121 \pm 32$  and  $91 \pm 34\%$  of Aph-1 $\alpha$ L, respectively (mean  $\pm$  S.D.,  $p > 0.05$ ). Values were corrected for Aph-1 incorporation into  $\gamma$ -secretase by normalizing to PS1 NTF co-immunoprecipitation levels. *D*, similar to *A*, but the lysates were precipitated for APP with the C-terminal directed antibody, C9, and blotted for APP (22C11), APP CTFs (C8), and Aph-1 (3F10).

generated that contained the mutations H171K, H197K, or H171K/H197K (double), and these were each stably expressed in P-22 cells. Lysates (1% CHAPSO) of these cells demonstrated that all three histidine mutant proteins were able to assemble into  $\gamma$ -secretase complexes, as all mutants led to an expression-dependent increase in mature NCT and PS NTF levels (Fig. 7A). In addition, when we immunoprecipitated these lysates for Aph-1, PS, or Pen-2, we confirmed that each of the histidine mutants could interact with the various members of  $\gamma$ -secretase (supplemental Fig. 5). Consistent with the previous report (28), we found that  $\gamma$ -secretases formed by these mutants were not active, as judged by their inability to decrease APP CTF levels like WT Aph-1 did (Fig. 7A, compare lanes 2–4 with 5–7). In addition, conditioned media from these cells showed that the histidine

mutants each led to less A $\beta$ -(1–40) secretion than with WT Aph-1 (supplemental Fig. 6).

Next, we assayed whether H171K, H197K, or H171K/H197K could associate with APP and its CTFs. DAPT-treated cell lysates (1% CHAPSO) were immunoprecipitated for Aph-1 and blotted for co-immunoprecipitation of APP. Mutants H171K and H197K had reduced binding to APP and APP CTF, and H171K/H197K had an even greater reduction in its association with APP and its CTF (Fig. 7B, lanes 7–10); however, all mutants retained their ability to bind mature NCT and PS NTF.

Finally, we examined the reverse co-immunoprecipitation and quantified the levels of Aph-1 that were co-immunoprecipitated by an APP antibody. Consistent with the Aph-1 immunoprecipitation (Fig. 7B), we observed a reduced association of the histidine mutants with APP (Fig. 7C). When the amounts of Aph-1 that co-immunoprecipitated with APP were normalized to their relative Aph-1 expression levels (*i.e.* the start), H171K, H197K, and H171K/H197K, respectively, bound APP at 59, 52, and 27% of the WT level (Fig. 7D). Together, our data suggest that the highly conserved TMD histidines His-171 and His-197 are important for substrate interaction (and therefore amount of cleavage) but may be dispensable for the assembly of the  $\gamma$ -secretase complex.

## DISCUSSION

Although  $\gamma$ -secretase is a complex of four distinct proteins that must act together to execute the unusual function of intramembrane proteolysis, recent studies have uncovered unique contributions of each cofactor to this function. For example, PS provides both aspartate residues necessary for the aspartyl-protease activity, essentially comprising the catalytic core of the enzyme (3). Pen-2 is thought to be the last component to enter into  $\gamma$ -secretase assembly and appears to induce a conformational change in the complex that enables PS endoproteolysis and thus the maturation of  $\gamma$ -secretase into an active enzyme (9–13). NCT has been reported to interact with the extreme N terminus of ectodomain-shed substrates immediately prior to  $\gamma$ -cleavage (4, 5); however, this remains unsettled (6). Although studies from our laboratory and others indicate that Aph-1 participates in bind-



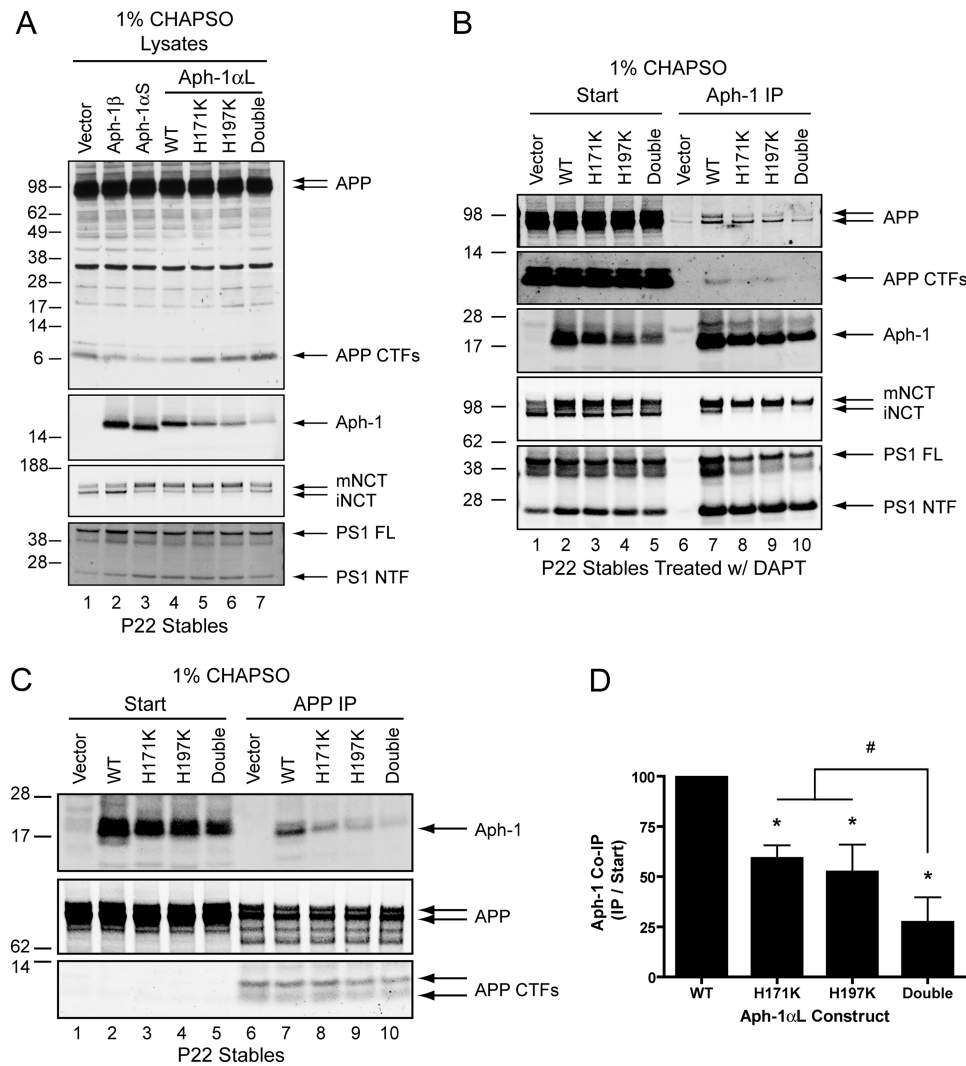


**FIGURE 7. Aph-1 residues His-171 and His-197 are involved in substrate binding.** *A*, P-22 cells were stably transfected to express either Aph-1 $\alpha$ L WT, H171K, H197K, or H171K/H197K (double). Cells were lysed and run alongside lysates of Aph-1 $\beta$  and Aph-1 $\alpha$ S stables in 1% CHAPSO and blotted for Aph-1 incorporation into  $\gamma$ -secretase via maturation of NCT (N1660) and PS1 NTF ( $\alpha$ -PS1 NT, Calbiochem) levels and for levels of APP CTFs (C7). *B*, to determine whether the Aph-1 histidine mutants can bind to APP and its CTFs, P-22 stables were treated with the  $\gamma$ -inhibitor, DAPT (2  $\mu$ M). Treated cells were lysed in 1% CHAPSO, immunoprecipitated (IP), and analyzed as in *A*. *C*, P-22 cells stably expressing vector, Aph-1 $\alpha$ L WT, H171K, H197K, or H171K/H197K (double) were lysed in 1% CHAPSO and precipitated for APP with affinity-purified antiserum C9. Immunoprecipitates were blotted for the co-immunoprecipitation of Aph-1 (3F10) and APP and APP CTF (22C11 and C7, respectively). *D*, quantification of *C* and several replicates thereof ( $n = 7$ ). H171K, H197K, and H171K/H197K mutants bound APP  $59 \pm 7$ ,  $52 \pm 14$ , and  $27 \pm 12\%$  of WT, respectively (mean  $\pm$  S.D.; \* indicates all mutants were significantly different from WT,  $p < 0.001$ ; # indicates double mutant was significantly different from each single mutant,  $p < 0.001$ ). Levels of Aph-1 immunoprecipitation were normalized to Aph-1 Start.

ing NCT early in the assembly of the complex (9, 13, 15, 42), a role for Aph-1 in  $\gamma$ -secretase proteolytic function is not established. It is of particular importance to examine Aph-1, as its seven transmembrane domains contribute almost half of the membrane-spanning motifs of the entire  $\gamma$ -complex.

Here, we provide multiple lines of evidence that Aph-1 plays a role in binding  $\gamma$ -secretase substrates, both the full-length holoproteins and their CTFs after the shedding of the ectodomains by  $\alpha$ -secretase. We first observed this in our  $\gamma$ -30 and S-20 CHO cell lines, in which Aph-1 was consistently found to be associated with the canonical  $\gamma$ -secretase substrate APP. This interaction was validated using two biochemical methods, co-immunoprecipitation (both directions) and cross-linking in

live cells. Even under  $\gamma$ -secretase denaturing conditions, we still observed a clear interaction between Aph-1 and the substrate APP. This could thus be seen in the absence of association with the other  $\gamma$ -components, ruling against the possibility that the Aph-1-substrate interaction is indirect and principally mediated by other  $\gamma$ -secretase cofactors. In addition, we were able to identify Aph-1-APP and Aph-1-APP CTF complexes using the detergent-independent method of live cell cross-linking, further supporting the notion that the interaction of Aph-1 with substrate occurs *in situ* and is not a product of a detergent-induced artifact. To control for nonspecific interactions between the hydrophobic Aph-1 and single-pass membrane proteins, we analyzed the type II protein, transferrin receptor, which is also overexpressed in our  $\gamma$ -30 cells. We found no evidence of an interaction between this highly expressed non-substrate and Aph-1. Most importantly, we validated the interaction at endogenous expression levels in both untransfected HEK cells and *in vivo* in mouse brain, in which multiple conditions consistently confirmed a specific interaction of Aph-1 with small amounts of APP holoprotein and its CTFs. Next, we demonstrated that an unrelated  $\gamma$ -secretase substrate, Jagged, interacts with Aph-1 in a similar manner at both overexpressed and endogenous levels, suggesting that the interaction may be a general step in the initial association of substrates with  $\gamma$ -secretase.

The binding between Aph-1 and  $\gamma$ -secretase substrates reported in this study is demonstrable in multiple systems, including in the brain *in vivo*, in various detergents, and in three different species (mouse, rat, and human), collectively supporting the occurrence of this interaction, which was unexpected by the field. Because there are two *APH-1* genes in humans and three in mice, and each has multiple splice variants that can participate in functionally active  $\gamma$ -secretase complexes (40), we examined whether the various isoforms can associate with substrate. We found that all Aph-1 isoforms tested (Aph-1 $\beta$ ,  $\alpha$ S, and  $\alpha$ L) were able to bind the  $\gamma$ -substrate APP with similar efficiency. This finding is consistent with a recent report that Aph-1 $\beta$  and Aph-1 $\alpha$  complexes appear to have indistinguishable kinetics for APP and Notch

## Aph-1 Binds to $\gamma$ -Secretase Substrates

cleavage ( $\epsilon$ -cleavage) (41), suggesting that their affinities for APP are similar. Finally, we attempted to map domains within Aph-1 that may be responsible for binding substrates. Using a previously published protocol of domain-swapping mutagenesis (11), we were able to generate seven Aph-1 mutants (except for TMD 4) with their TMDs swapped with the TMD of an unrelated protein. Unfortunately, all of the mutants incorporated poorly into  $\gamma$ -secretase, as assayed by mature complex assembly and association with NCT and PS, so they could not be studied further. Next, we examined two highly conserved histidine residues within TMD5 and -6, which were recently shown to be important for  $\gamma$ -secretase activity (28). We generated Aph-1 $\alpha$ L mutants H171K, H197K, and a double mutant and tested them for both incorporation into  $\gamma$ -secretase and binding to APP. We were able to reproduce the previous report, as all three histidine mutants incorporated into  $\gamma$ -secretase similarly to WT Aph-1, but the complexes appeared inactive, as APP CTFs levels were elevated and less A $\beta$  was generated when compared with WT Aph-1. Each single mutant associated with APP less than WT Aph-1, and the double mutant exhibited an even greater deficit, suggesting that both histidines are individually involved in this interaction. These substrate-binding data could explain why complexes containing these histidine mutants are inactive. Together, these data suggest that histidines 171 and 197 may play a critical role in the association of substrates with  $\gamma$ -secretase.

It was reported previously that NCT can bind to the extreme N terminus of immediate substrates (*i.e.* CTFs) within  $\gamma$ -secretase (4). Our new data suggest that Aph-1 can bind full-length substrates in addition to binding the ectodomain-shed CTF substrates, even in the absence of association with NCT (*e.g.* in 1% Nonidet P-40). Although we did not obtain clear-cut evidence for an independent interaction between APP and NCT, we cannot rule this out, because the interaction could be highly transient and difficult to detect under our conditions. However, under both overexpressed and endogenous conditions, our data reveal a more robust interaction of substrates with Aph-1 than with NCT. These results suggest that Aph-1 may interact with a full-length substrate prior to ectodomain shedding and the docking of the CTF with NCT. It is possible that NCT and Aph-1 may together form the substrate-docking site once the ectodomain is shed, because Aph-1 and NCT are known to interact tightly with one another and form a stable subcomplex (15, 18), as we also observed here.

As we observed interactions not only with CTFs but also full-length substrates that are not the immediate targets of  $\gamma$ -secretase, one possible role is that Aph-1 maintains full-length substrates that are about to have their ectodomains shed by  $\alpha$ -secretases within the  $\gamma$ -complex, facilitating subsequent association of the CTFs with the apparent NCT/PS-docking site (4, 43) and then entry into the catalytic site. An additional possibility is that Aph-1 functions in the binding and trafficking of holoproteins destined to become substrates to the vesicles or membrane microdomains in which the mature protease acts.

Our data here are consistent with emerging data in the field that Aph-1 is intimately involved in the proteolytic processing of substrates by  $\gamma$ -secretase. A recent report has shown that  $\gamma$ -secretase complexes containing Aph-1 $\beta$  generate longer A $\beta$

peptides compared with complexes containing Aph-1 $\alpha$  (41). Interestingly, His-197, which we believe to be involved in substrate interaction, is shifted within TM6 of Aph-1 $\beta$  as compared with Aph-1 $\alpha$ , which may help explain this phenomenon. This study (41) also found that ablation of the *Aph-1 $\beta$*  gene rescued AD-like phenotypes in APP-overexpressing mice without detectable interference with Notch cleavage, suggesting that various Aph-1-containing  $\gamma$ -secretase complexes participate in somewhat different protein processing events *in vivo*. Indeed, it appears that the various Aph-1-containing  $\gamma$ -complexes may have somewhat different physiological substrates *in vivo* (44–46) further supporting a role of Aph-1 in substrate processing. Finally, mutants in Aph-1 have been shown to inactivate proteolytic processing by  $\gamma$ -secretase while sparing its complex assembly (28). Here, we propose that Aph-1 involvement in  $\gamma$ -secretase processing is due to its role as a substrate-binding moiety within the  $\gamma$ -complex.

---

*Acknowledgments*—We thank Dr. Michael S. Wolfe (Brigham and Women's Hospital and Harvard Medical School) for DAPT and a critical reading of the manuscript, Drs. Dominic Walsh (University College Dublin) and Patrick Fraering (EPFL, Brain Mind Institute) for helpful discussions, and Wenjuan Ye for technical assistance.

---

## REFERENCES

1. Beel, A. J., and Sanders, C. R. (2008) *Cell. Mol. Life Sci.* **65**, 1311–1334
2. Selkoe, D. J., and Wolfe, M. S. (2007) *Cell* **131**, 215–221
3. Wolfe, M. S., Xia, W., Ostaszewski, B. L., Diehl, T. S., Kimberly, W. T., and Selkoe, D. J. (1999) *Nature* **398**, 513–517
4. Shah, S., Lee, S. F., Tabuchi, K., Hao, Y. H., Yu, C., LaPlant, Q., Ball, H., Dann, C. E., 3rd, Südhof, T., and Yu, G. (2005) *Cell* **122**, 435–447
5. Dries, D. R., Shah, S., Han, Y. H., Yu, C., Yu, S., Shearman, M. S., and Yu, G. (2009) *J. Biol. Chem.* **284**, 29714–29724
6. Chávez-Gutiérrez, L., Tolia, A., Maes, E., Li, T., Wong, P. C., and de Strooper, B. (2008) *J. Biol. Chem.* **283**, 20096–20105
7. Shirovani, K., Edbauer, D., Kostka, M., Steiner, H., and Haass, C. (2004) *J. Neurochem.* **89**, 1520–1527
8. Futai, E., Yagishita, S., and Ishiura, S. (2009) *J. Biol. Chem.* **284**, 13013–13022
9. Takasugi, N., Tomita, T., Hayashi, I., Tsuruoka, M., Niimura, M., Takahashi, Y., Thinakaran, G., and Iwatsubo, T. (2003) *Nature* **422**, 438–441
10. Prokop, S., Shirovani, K., Edbauer, D., Haass, C., and Steiner, H. (2004) *J. Biol. Chem.* **279**, 23255–23261
11. Watanabe, N., Tomita, T., Sato, C., Kitamura, T., Morohashi, Y., and Iwatsubo, T. (2005) *J. Biol. Chem.* **280**, 41967–41975
12. Kim, S. H., and Sisodia, S. S. (2005) *J. Biol. Chem.* **280**, 41953–41966
13. Luo, W. J., Wang, H., Li, H., Kim, B. S., Shah, S., Lee, H. J., Thinakaran, G., Kim, T. W., Yu, G., and Xu, H. (2003) *J. Biol. Chem.* **278**, 7850–7854
14. Fortna, R. R., Crystal, A. S., Morais, V. A., Pijak, D. S., Lee, V. M., and Doms, R. W. (2004) *J. Biol. Chem.* **279**, 3685–3693
15. LaVoie, M. J., Fraering, P. C., Ostaszewski, B. L., Ye, W., Kimberly, W. T., Wolfe, M. S., and Selkoe, D. J. (2003) *J. Biol. Chem.* **278**, 37213–37222
16. Capell, A., Behr, D., Prokop, S., Steiner, H., Kaether, C., Shearman, M. S., and Haass, C. (2005) *J. Biol. Chem.* **280**, 6471–6478
17. Lee, S. F., Shah, S., Li, H., Yu, C., Han, W., and Yu, G. (2002) *J. Biol. Chem.* **277**, 45013–45019
18. Hu, Y., and Fortini, M. E. (2003) *J. Cell Biol.* **161**, 685–690
19. Morais, V. A., Crystal, A. S., Pijak, D. S., Carlin, D., Costa, J., Lee, V. M., and Doms, R. W. (2003) *J. Biol. Chem.* **278**, 43284–43291
20. Xia, W., Zhang, J., Perez, R., Koo, E. H., and Selkoe, D. J. (1997) *Proc. Natl. Acad. Sci. U.S.A.* **94**, 8208–8213
21. Xia, W., Zhang, J., Ostaszewski, B. L., Kimberly, W. T., Seubert, P., Koo, E. H., Shen, J., and Selkoe, D. J. (1998) *Biochemistry* **37**, 16465–16471

22. Ray, W. J., Yao, M., Nowotny, P., Mumm, J., Zhang, W., Wu, J. Y., Kopan, R., and Goate, A. M. (1999) *Proc. Natl. Acad. Sci. U.S.A.* **96**, 3263–3268
23. Ray, W. J., Yao, M., Mumm, J., Schroeter, E. H., Saftig, P., Wolfe, M., Selkoe, D. J., Kopan, R., and Goate, A. M. (1999) *J. Biol. Chem.* **274**, 36801–36807
24. Xia, W., Ray, W. J., Ostaszewski, B. L., Rahmati, T., Kimberly, W. T., Wolfe, M. S., Zhang, J., Goate, A. M., and Selkoe, D. J. (2000) *Proc. Natl. Acad. Sci. U.S.A.* **97**, 9299–9304
25. LaVoie, M. J., and Selkoe, D. J. (2003) *J. Biol. Chem.* **278**, 34427–34437
26. Berezovska, O., Ramdya, P., Skoch, J., Wolfe, M. S., Bacskai, B. J., and Hyman, B. T. (2003) *J. Neurosci.* **23**, 4560–4566
27. Esler, W. P., Kimberly, W. T., Ostaszewski, B. L., Ye, W., Diehl, T. S., Selkoe, D. J., and Wolfe, M. S. (2002) *Proc. Natl. Acad. Sci. U.S.A.* **99**, 2720–2725
28. Pardossi-Piquard, R., Yang, S. P., Kanemoto, S., Gu, Y., Chen, F., Böhm, C., Sevalle, J., Li, T., Wong, P. C., Checler, F., Schmitt-Ulms, G., St George-Hyslop, P., and Fraser, P. E. (2009) *J. Biol. Chem.* **284**, 16298–16307
29. Kimberly, W. T., LaVoie, M. J., Ostaszewski, B. L., Ye, W., Wolfe, M. S., and Selkoe, D. J. (2003) *Proc. Natl. Acad. Sci. U.S.A.* **100**, 6382–6387
30. Fraering, P. C., Ye, W., Strub, J. M., Dolios, G., LaVoie, M. J., Ostaszewski, B. L., van Dorsselaer, A., Wang, R., Selkoe, D. J., and Wolfe, M. S. (2004) *Biochemistry* **43**, 9774–9789
31. Hemming, M. L., Patterson, M., Reske-Nielsen, C., Lin, L., Isacson, O., and Selkoe, D. J. (2007) *PLoS Med.* **4**, e262
32. Zheng, H., Jiang, M., Trumbauer, M. E., Sirinathsinghji, D. J., Hopkins, R., Smith, D. W., Heavens, R. P., Dawson, G. R., Boyce, S., Conner, M. W., Stevens, K. A., Slunt, H. H., Sisoda, S. S., Chen, H. Y., and Van der Ploug, L. H. (1995) *Cell* **81**, 525–531
33. Kimberly, W. T., Zheng, J. B., Town, T., Flavell, R. A., and Selkoe, D. J. (2005) *J. Neurosci.* **25**, 5533–5543
34. Fraering, P. C., LaVoie, M. J., Ye, W., Ostaszewski, B. L., Kimberly, W. T., Selkoe, D. J., and Wolfe, M. S. (2004) *Biochemistry* **43**, 323–333
35. Cacquevel, M., Aeschbach, L., Osenkowski, P., Li, D., Ye, W., Wolfe, M. S., Li, H., Selkoe, D. J., and Fraering, P. C. (2008) *J. Neurochem.* **104**, 210–220
36. Steiner, H., Winkler, E., and Haass, C. (2008) *J. Biol. Chem.* **283**, 34677–34686
37. Struhl, G., and Adachi, A. (2000) *Mol. Cell* **6**, 625–636
38. Ikeuchi, T., and Sisodia, S. S. (2003) *J. Biol. Chem.* **278**, 7751–7754
39. Lindsell, C. E., Boulter, J., diSibio, G., Gossler, A., and Weinmaster, G. (1996) *Mol. Cell. Neurosci.* **8**, 14–27
40. Shirohani, K., Edbauer, D., Prokop, S., Haass, C., and Steiner, H. (2004) *J. Biol. Chem.* **279**, 41340–41345
41. Serneels, L., Van Biervliet, J., Craessaerts, K., Dejaegere, T., Horr , K., Van Houtvin, T., Esselmann, H., Paul, S., Sch fer, M. K., Berezovska, O., Hyman, B. T., Sprangers, B., Sciot, R., Moons, L., Jucker, M., Yang, Z., May, P. C., Karran, E., Wiltfang, J., D'Hooge, R., and De Strooper, B. (2009) *Science* **324**, 639–642
42. Gu, Y., Chen, F., Sanjo, N., Kawarai, T., Hasegawa, H., Duthie, M., Li, W., Ruan, X., Luthra, A., Mount, H. T., Tandon, A., Fraser, P. E., and St George-Hyslop, P. (2003) *J. Biol. Chem.* **278**, 7374–7380
43. Kornilova, A. Y., Bihel, F., Das, C., and Wolfe, M. S. (2005) *Proc. Natl. Acad. Sci. U.S.A.* **102**, 3230–3235
44. Coolen, M. W., van Loo, K. M., van Bakel, N. N., Ellenbroek, B. A., Cools, A. R., and Martens, G. J. (2006) *FASEB J.* **20**, 175–177
45. Dejaegere, T., Serneels, L., Sch fer, M. K., Van Biervliet, J., Horr , K., Depboylu, C., Alvarez-Fischer, D., Herreman, A., Willem, M., Haass, C., H glinger, G. U., D'Hooge, R., and De Strooper, B. (2008) *Proc. Natl. Acad. Sci. U.S.A.* **105**, 9775–9780
46. Coolen, M. W., Van Loo, K. M., Van Bakel, N. N., Pulford, D. J., Serneels, L., De Strooper, B., Ellenbroek, B. A., Cools, A. R., and Martens, G. J. (2005) *Neuron* **45**, 497–503